3-17-2017

Analysis of an Upper Bound on the Effects of Large Scale Attenuation on Uplink Transmission Performance for Massive MIMO Systems

Liu Liu

David W. Matolak
University of South Carolina - Columbia, matolak@cec.sc.edu

Cheng Tao

Yongzhi Li

Publication Info

Published in *IEEE Access*, Volume 5, 2017, pages 4285-4297.

IEEE Access
Multidisciplinary | Rapid Review | Open Access Journal

Received February 25, 2017, accepted accepted March 15, 2017, date of publication March 17, 2017, date of current version April 24, 2017.

Digital Object Identifier 10.1109/ACCESS.2017.2684089

Analysis of an Upper Bound on the Effects of Large Scale Attenuation on Uplink Transmission Performance for Massive MIMO Systems

LIU LIU[1,2], (Member, IEEE), DAVID W. MATOLAK[3], (Senior Member, IEEE), CHENG TAO[1,2], (Member, IEEE), AND YONGZHI LI[1]

[1]School of Electronic and Information Engineering, Institute of Broadband Wireless Mobile Communications, Beijing Jiaotong University, Beijing 100044, China
[2]National Mobile Communications Research Laboratory, Southeast University, Nanjing, 211189, China
[3]Department of Electrical Engineering, University of South Carolina, Columbia, SC 29208, USA

Corresponding author: L. Liu (liuliu@bjtu.edu.cn)

This work was supported in part by the Beijing Nova Programme under Grant Z161100004916068, in part by the Fundamental Research Funds for the Central Universities under Grant 2017JBM306, in part by NSFC Project under Grant 61471027, in part by the Research Fund of National Mobile Communications Research Laboratory, Southeast University, under Grant 2014D05 and Grant 2017D01, and in part by the Beijing Natural Science Foundation Project under Grant 4152043. This paper was presented at the 2016 IEEE 84th Vehicular Technology Conference.

ABSTRACT Massive multiple-input multiple-output (MIMO) is a potential candidate key technology for the 5G of wireless communication systems. In research to date, different power loss and shadowing effects on different antenna elements across the large arrays have been neglected. In this paper, based on an idealized propagation model, a new large scale attenuation (LSA) model is proposed, by which the large scale losses (path loss and shadowing effect) over the antenna array can be considered when establishing a massive MIMO channel model. By using this model, the spectral efficiency (in terms of bits/s/Hz sum-rate) of the maximum ratio combining (MRC) detector is derived for the uplink. The spectral efficiency performance of the zero forcing (ZF) detector also can be derived in the same manner. It can be found that the sum-rate performance (MRC and ZF) of our proposed channel model (assuming independent shadowing on all elements of the array) exceeds that of the conventional model (where the LSA effect is not included). Based upon our theoretical and simulation analysis, we have found that the spectral efficiency gap is mainly from the mean value of different shadowing effects across different elements, and the different path losses experienced by different antenna elements provide negligible contribution. This LSA model and the derived performance results could be beneficial and informative for the research, design and evaluation of the next generation of wireless communication system employing a massive MIMO configuration.

INDEX TERMS Massive MIMO, large scale attenuation, path loss, shadowing effect, sum-rate.

I. INTRODUCTION

Massive MIMO, or large-scale MIMO, is a recently proposed technique for future wireless communication systems. It can provide high data throughput and high power efficiency, and improve the communication reliability with fairly simple signal processing. By equipping each base-station (BS) with an antenna array of a large number of (e.g., more than 100) antenna elements, and each user terminal with one, or likely no more than two antenna elements, channel coefficient vectors can become asymptotically orthogonal(as the number of BS elements gets large). Under this condition, the matched filter achieves nearly optimal performance at the BS. The multiuser interference is effectively canceled, and signal-to-noise ratio (SNR) is dramatically enhanced [1].

In order to evaluate the performance of massive MIMO systems, accurate channel models are vital. In [1] and [2], the fading channel of a massive MIMO system is characterized by multiplying two matrices $\mathbf{H}_{M\times K}$ and $\mathbf{D}_{K\times K}$ to obtain $\mathbf{G}_{M\times K} = \mathbf{H}\mathbf{D}^{1/2}$, where M is the number of antenna elements at the BS, K is the number of users, $\mathbf{H}$ accounts for the small scale fading gain (SSFG), and the diagonal matrix $\mathbf{D}$ accounts for the large scale attenuation (LSA). Based on this cascaded channel model, the transmission capacity, the energy and spectral efficiency, the performance of pre-coding

methods are investigated in [1], [2] and [3]. In the so-called "favorable propagation condition" [1], [2] and [4], channel coefficient vectors $\mathbf{h}_i = \left[h_{i,1}, h_{i,2}, \cdots, h_{i,M}\right]^T$ and $\mathbf{h}_j = \left[h_{j,1}, h_{j,2}, \cdots, h_{j,M}\right]^T$ ($h_{i,m}$ is the ith user's small scale fading channel to BS element m) whose elements are independent identically distributed (i.i.d.) zero-mean random variables with unit variance, generate the small scale fading matrix $\mathbf{H}$. By using the strong law of large numbers (the number of BS antenna elements grows indefinitely large), we obtain the asymptotic result as $\frac{\mathbf{G}^H\mathbf{G}}{M} = \mathbf{D}^{1/2}\frac{\mathbf{H}^H\mathbf{H}}{M}\mathbf{D}^{1/2} \approx \mathbf{D}$ ($M \gg K$), where $(\cdot)^H$ denotes the Hermitian transpose operation. Under this condition, the small scale fading effect is removed, and the remaining term of the matrix product is the LSA matrix $\mathbf{D}$. This means that a large number of antennas effectively could only eliminate the small-scale fading, but the large scale fading effect still remains. In [1] and [2], it was shown that the LSA matrix $\mathbf{D}$ (including path loss and shadowing) eventually determines the final sum-rate capacity expressions of multiuser massive MIMO systems, for both the forward link and the reverse link, and the optimal transmit power for each user is determined by the LSA, not by the SSFG. This effect can be termed the channel hardening phenomenon as in [5] and [6]. The channel hardening effect can mitigate the impact of small scale fading on the scheduling gain, and thus subsequent performance investigation should focus on the large scale fading.

In a practical massive MIMO antenna system, the size of the antenna structure is substantially enlarged compared with conventional compact multiple antenna systems, especially for the one-dimensional linear antenna array. The linear antenna array is selected for investigation in this paper. For a given number of antenna elements, the linear array has the largest antenna size. We select this array shape because the signals transmitted from different elements or impinging upon different elements are more likely to experience different power attenuation (path loss and shadowing) when the array size is largest. We term this the LSA effect over the antenna array. It can be observed that different power attenuation values (due to different propagation distances) and different shadowing values (due to different geometries with respect to obstructions) can be incurred by different antenna elements on the antenna array. This effect has also been noted in [7]–[10]. However, in most of the literature, the large-scale fading effect is ignored and simply assumed constant for simplicity, i.e., in the neglected LSA case $\mathbf{D} = \mathbf{I}_K$ ($\mathbf{I}_K$ is a $K \times K$ identity matrix), or the diagonal elements of the squared LSA matrix $\mathbf{D}$ are assumed to be constant. By using this simplified large scale model, the system performance result will not be accurate.

To date, there has been an ever-increasing body of research results for massive MIMO channels. In [8], received power variation along the antenna array was actually observed. In [10], a geometry based large scale fading model was first proposed to characterize the power attenuation over a linear antenna array. In [11], the time delay spread properties in line-of-sight (LOS) and non line-of-sight (NLOS) massive MIMO scenarios were studied. In [12], the fading behavior and spatial correlation properties on large arrays in different propagation environments were analyzed. In [13], the achievable performance of two types of antenna arrays were investigated based on realistic measurement data. In [14], a composite channel model considering the large and small scale fading was used to analyze the ergodic achievable rate of a large uplink massive MIMO system. However, few investigations have been done on large scale fading characteristics over massive MIMO arrays, especially for the performance analysis considering specifically the LSA effect.

The main contribution of this paper is to establish a reference large scale attention model, and investigate the uplink transmission performance.

- Based on basic propagation principles, we establish a new large scale attention (LSA) model that can serve as a useful reference to describe the large scale fading over the antenna array. In this LSA model, the power loss and shadowing effects of each propagation ray are individually quantified. The final cascaded channel matrix is generated by a Hadamard product of a LSA matrix and a small scale fading matrix.
- By using the proposed LSA model, we show that the channel hardening effect that yields a constant large scale fading value in $\mathbf{D}$ is thus changed to the mean value of the large scale fading coefficients (path loss and shadowing) on individual antenna elements over the antenna array. We derive closed-form expressions of the sum-rate capacity for MRC under perfect and imperfect channel estimation (or channel state information (CSI)) conditions. In the same manner, results for ZF and MMSE also can be obtained.
- From our investigation, it can be found that the sum-rate performance (MRC and ZF) of our proposed channel model is better than that of the conventional model (where the LSA effect is not included). As for the LSA model, the power loss difference caused by the physical size of the antenna array is negligible, and the performance gap arises from the mean value of the randomly distributed shadowing samples on different antenna elements. Simulation results are provided to verify our conclusions in this paper.
- Although we use the ideal case that independent (different) random shadowing values occur on each individual element on the antenna array, this assumption does not represent a practical case (because the shadowing effects from adjacent elements may be correlated), it provides insight into the effects of LSA on capacity that are useful to know.

The rest of the paper is organized as follows. Section II describes the system and proposes an extended LSA matrix which contains the large-scale fading over the antenna array. In Section III, closed-form expressions of the sum-rate capacity for MRC under perfect and imperfect channel estimation conditions are derived, and then we analyze the

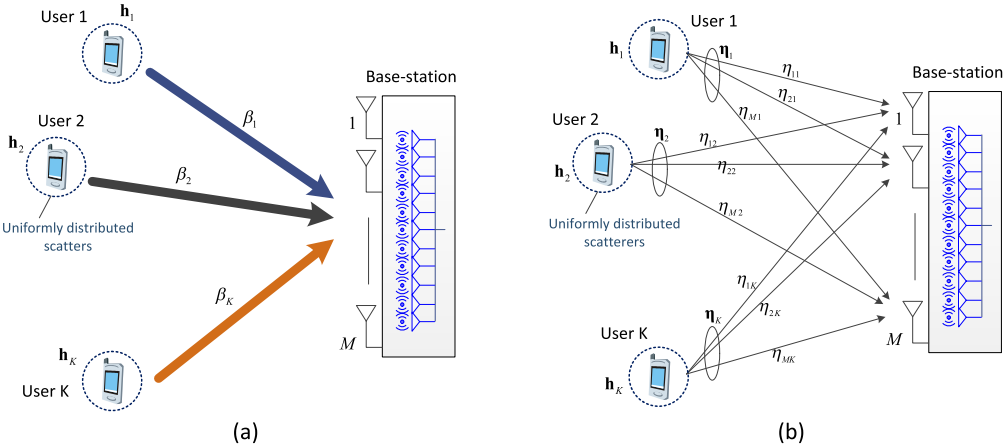

FIGURE 1. A comparison of propagation environments. (a) The conventional propagation model, and (b) The LSA model.

statistical characteristics between the large-scale fading effect and deduce the transmission difference of our LSA model and the conventional model in Section IV. The verifying simulation results are present in Section V, and conclusions are drawn in Section VI.

II. SYSTEM DESCRIPTIONS

In this paper, we consider the uplink transmission of a multiuser massive MIMO system. The BS, equipped with a linear array of M antennas, receives the signal from K single-antenna users simultaneously. The conventional propagation environment is illustrated in Figure 1 (a). This conventional model can be found in [2].

The users transmit their data in the same narrowband time-frequency resource. At the BS, the $M \times 1$ received vector $\mathbf{y}$ can be expressed as

$$\mathbf{y} = \sqrt{p_u}\mathbf{G}\mathbf{s} + \mathbf{n}, \tag{1}$$

where $\mathbf{s}_{K\times 1}$ is the vector of signals simultaneously transmitted by K users, the average transmitted power of each user is p_u (Here we assume all users are perfectly power controlled to have the same power at the BS), and $\mathbf{n}$ is a vector of additive white, zero-mean Gaussian noise. The channel matrix $\mathbf{G}$ characterizes the independent small scale fading, path loss, and log-normal shadow fading. The coefficient g_{mk} in $\mathbf{G}$ can be written in a composite form as

$$g_{mk} = h_{mk}\sqrt{\beta_k}, \quad m = 1, 2, \cdots, M, \tag{2}$$

where h_{mk} is the small scale fading coefficient from the kth user to the mth antenna of the BS, $\sqrt{\beta_k}$ models the power attenuation and shadow fading, and the value of β_k changes very slowly with time. Then, we have

$$\mathbf{G} = \mathbf{H}\mathbf{D}^{1/2}, \tag{3}$$

where $\mathbf{H}$ is the $M \times K$ matrix of small scale fading coefficients between the K users and the BS. Its ith column vector $\mathbf{h}_i = \left[h_{i,1}, h_{i,2}, \cdots, h_{i,M}\right]^T$ is composed of i.i.d. zero-mean complex Gaussian random variables with unit variance. $\mathbf{D}$ is a $K \times K$ diagonal matrix, where $[\mathbf{D}]_{kk} = \beta_k$.

A. LARGE SCALE ATTENUATION CHANNEL MATRIX

Up to now, in most massive MIMO research, the large-scale fading effect is ignored or simply assumed constant for simplicity, i.e., $\mathbf{D} = \mathbf{I}_K$ ($\mathbf{I}_K$ is a $K \times K$ unitary matrix), or the large scale attenuation matrix $\mathbf{D}$ is a diagonal square matrix of distance-dependent constants. However, in practice, as observed from measurement results, we can see that when the size of the antenna-array is large, especially for the one-dimensional array, different large scale fading effects occur over the antenna array [10]. To characterize the propagation more accurately, the large scale propagation properties between the user and each antenna element should be considered separately. Theoretically, each element in a physically large structure will receive the arriving signals with different strengths. This variation can be attributed to different propagation path lengths and the variation of geometry of shadowing effects over the antenna array. The propagation rays are as shown in Figure 1 (b).

Here, we use the common log-distance model to investigate the signal variation between the specific user terminal and BS antenna element, and the path loss (PL) in decibels is determined by the transmission distance in meters r, the path loss exponent n and the Gaussian distributed shadowing term X_{dB} with zero mean value and standard deviation of σ [15]. In this PL log-distance model, there is a reference distance r_0 (r_0 depends on the coverage area of a particular cellular system, e.g., typically it is 1 m for small cells). In [2], r_0 denotes the minimum range from the BS of a user terminal.

In the linear scale, the large scale fading coefficient is given as[1]

$$\frac{P_R(r)}{P_T} = \frac{c_0 \cdot (r_0)^n}{x \cdot (r)^n} \; or \; \frac{x \cdot c_0 \cdot (r_0)^n}{(r)^n}, \tag{4}$$

[1] In [2] and [14], the large scale fading gain is expressed as $p_R(r)/p_T = c_0 x/(r/r_0)^n$, in which the shadowing term is part of the numerator. This is equivalent because the shadowing effect X is characterized as the zero mean Gaussian variable. An addition or subtraction of zero-mean symmetrically distributed X in the path loss model of (4) yields the same effect.

where the lognormal shadowing value $x = 10^{\frac{X}{10}}$, $c_0 = 10^{-\frac{PL(r_0)}{10}}$ is the mean path gain at reference distance r_0. c_0 is a constant value that also depends on the carrier frequency, the antenna gain and the speed of light. Here we assume that c_0 can be perfectly compensated when planning the link budget, and thus the distance-dependent large scale fading coefficient η_{mk} between the kth user and mth antenna element can be obtained

$$\eta_{mk} = x_{mk} \cdot \frac{(r_0)^n}{(r_{mk})^n}. \tag{5}$$

When an M-element massive MIMO system serves K users in the cell, and taking the large scale fading over the antenna array into account, the squared LSA matrix $\mathbf{D}$ $(K \times K)$ changes into a tall shape matrix $\dot{\mathbf{D}}$ $(M \times K)$ as

$$\dot{\mathbf{D}} = \begin{bmatrix} \eta_{11} & \eta_{12} & \cdots & \eta_{1K} \\ \eta_{21} & \eta_{22} & \cdots & \eta_{2K} \\ \vdots & \vdots & & \vdots \\ \eta_{M1} & \eta_{M2} & \cdots & \eta_{MK} \end{bmatrix} = \begin{bmatrix} \boldsymbol{\eta}_1 & \boldsymbol{\eta}_2 & \cdots & \boldsymbol{\eta}_K \end{bmatrix}, \tag{6}$$

where $\eta_{mk} (1 \le m \le M, 1 \le k \le K)$ is the LSA of the mth antenna element on the array for the kth user, and the column vector $\boldsymbol{\eta}_k$ in $\dot{\mathbf{D}}$ describes the large scale fading of the kth user. Then the cascaded fading matrix will be changed as

$$\dot{\mathbf{G}} = \mathbf{H} \circ \left(\dot{\mathbf{D}}\right)^{1/2}, \tag{7}$$

where $\circ$ is the Hadamard product. For two matrices, $\mathbf{A}$ and $\mathbf{B}$, $\mathbf{A} \circ \mathbf{B}$ is a matrix with elements given by $(\mathbf{A} \circ \mathbf{B})_{i,j} = (\mathbf{A})_{i,j} \cdot (\mathbf{B})_{i,j}$. Compared with the conventional model ($\mathbf{D} = \mathbf{I}_K$) and the simplified path loss model (the diagonal element of $\mathbf{D}$ is $(\mathbf{D})_i = x/(r_i)^n$ in [2] and [14], this novel reference LSA accounts for the large scale fading over the antenna array as part of the fading coefficients of the propagation channel. It can provide a more accurate channel description for massive MIMO systems, especially for the one-dimensional linear antenna array.

B. INNER PRODUCT OF CHANNEL VECTORS CONSIDERING THE LSA EFFECT

In the conventional model of (3), by using the law of large numbers, we can obtain [1] and [2]

$$\frac{1}{M} (\mathbf{g}_k)^H (\mathbf{g}_l) \xrightarrow{M \to \infty} E\left[(\mathbf{g}_k)^H (\mathbf{g}_l)\right] = \begin{cases} 0, & k \ne l \\ \beta_k, & k = l. \end{cases} \tag{8}$$

When the propagation channel matrix accounts for the LSA effect, for a certain user k, the LSA based propagation vector $\dot{\mathbf{g}}_k$ (the kth column in $\dot{\mathbf{G}}$) can be expressed as

$$\begin{aligned} \dot{\mathbf{g}}_k &= \mathbf{h}_k \circ \left(\boldsymbol{\eta}_k\right)^{1/2} \\ &= \left[\sqrt{\eta_{1k}} h_{1k}, \sqrt{\eta_{2k}} h_{2k}, \cdots, \sqrt{\eta_{Mk}} h_{Mk}\right]^T. \end{aligned} \tag{9}$$

Then the inner product of LSA channel vectors is

$$(\dot{\mathbf{g}}_k)^H (\dot{\mathbf{g}}_l) = \begin{cases} \sum_{m=1}^{M} \sqrt{\eta_{mk}\eta_{ml}} \cdot h_{mk}^* \cdot h_{ml}, & k \ne l \\ \sum_{m=1}^{M} \eta_{mk} \cdot |h_{mk}|^2, & k = l. \end{cases} \tag{10}$$

By using the law of large numbers, we have

$$\begin{aligned} &\frac{1}{M} (\dot{\mathbf{g}}_k)^H (\dot{\mathbf{g}}_l) \xrightarrow{M \to \infty} E\left[(\dot{\mathbf{g}}_k)^H (\dot{\mathbf{g}}_l)\right] \\ &= \begin{cases} E\left[\sum_{m=1}^{M} \sqrt{\eta_{mk}\eta_{ml}} \cdot h_{mk}^* \cdot h_{ml}\right] = 0, & k \ne l \\ E\left[\sum_{m=1}^{M} \eta_{mk} \cdot |h_{mk}|^2\right] = \frac{1}{M} \sum_{m=1}^{M} \eta_{mk}, & k = l. \end{cases} \end{aligned} \tag{11}$$

According to (7) - (11), we can obtain eq.(13) on the top of the next page, where $\eta_k = \sum_{m=1}^{M} \eta_{mk}$. Compared with the conventional model, we can see that the main difference of our proposed LSA model is the summation term $\frac{1}{M} \sum_{m=1}^{M} \eta_{mk}$. As for the kth user, if the large scale coefficients (path loss and shadowing) over the antenna array are nearly the same, then we can obtain $\beta_k = \eta_{1k} = \eta_{2k} = \cdots \eta_{Mk}$. In this case, the Euclidean norm of the LSA channel matrix, $\frac{1}{M} \dot{\mathbf{G}}^H \dot{\mathbf{G}}$, changes into the result of the conventional model as eq.(14) on the top of the next page.

Meanwhile, the conventional model $\mathbf{G} = \mathbf{H}\mathbf{D}^{1/2}$ also can be expressed using our LSA model formulation (we term this the LSA based conventional model hereafter). Because the large scale attenuation values on the antenna array in the conventional model are the same, the LSA matrix $\dot{\mathbf{D}}$ can be expressed as

$$\begin{aligned} \dot{\mathbf{D}} &= \begin{bmatrix} \eta_{11} & \eta_{12} & \cdots & \eta_{1K} \\ \eta_{21} & \eta_{22} & \cdots & \eta_{2K} \\ \vdots & \vdots & & \vdots \\ \eta_{M1} & \eta_{M2} & \cdots & \eta_{MK} \end{bmatrix} \\ &= \begin{bmatrix} \beta_1 & \beta_2 & \cdots & \beta_K \\ \beta_1 & \beta_2 & \cdots & \beta_K \\ \vdots & \vdots & & \vdots \\ \beta_1 & \beta_2 & \cdots & \beta_K \end{bmatrix}_{M \times K}, \end{aligned} \tag{15}$$

where elements in all rows of any column vectors in $\dot{\mathbf{D}}$ are equal, that is $\dot{\mathbf{D}}$ $(1 \le m \le M, 1 \le k \le K)$.

III. ACHIEVABLE RATE PERFORMANCE ANALYSIS CONSIDERING THE LSA EFFECT

In [2], the researchers derived results for the achievable rate of the uplink, under perfect channel state information (CSI) and imperfect CSI at the BS. These results are based on an assumption that there is no LSA effect on the large scale antenna array. In practice, the different LSA on different antenna elements can substantially affect the final result.

$$E\left(\dot{\mathbf{G}}^H\dot{\mathbf{G}}\right)\xrightarrow{M\to\infty}\frac{1}{M}\dot{\mathbf{G}}^H\dot{\mathbf{G}}=\begin{bmatrix}\frac{1}{M}\sum_{m=1}^{M}\eta_{m1} & & 0\\ & \ddots & \\ 0 & & \frac{1}{M}\sum_{m=1}^{M}\eta_{mK}\end{bmatrix}=\frac{1}{M}\begin{bmatrix}\eta_1 & & 0\\ & \ddots & \\ 0 & & \eta_K\end{bmatrix}=\frac{1}{M}\boldsymbol{\eta} \tag{13}$$

$$\frac{1}{M}\begin{bmatrix}\eta_1 & & 0\\ & \ddots & \\ 0 & & \eta_K\end{bmatrix}_{K\times K}=\frac{1}{M}\begin{bmatrix}\sum_{m=1}^{M}\eta_{m1} & & 0\\ & \ddots & \\ 0 & & \sum_{m=1}^{M}\eta_{mK}\end{bmatrix}=\begin{bmatrix}\beta_1 & & 0\\ & \ddots & \\ 0 & & \beta_K\end{bmatrix} \tag{14}$$

In this section, we extend the analytical results of the achievable rate using the MRC linear detector considering the LSA effect on the antenna array. We will show that there can be a fairly large gap between the results from the conventional model and the reference LSA model - specifically, there is a substantial performance gain when using this LSA model. Other linear detection techniques, e.g. ZF, MMSE, can be assessed in a similar way.

A. ACHIEVABLE RATE ($M \to \infty$) WITH PERFECT CSI AT THE BS

We first consider the case when the BS can obtain perfect CSI, i.e. the BS can extract the channel matrix $\mathbf{G}$ (or $\dot{\mathbf{G}}$) perfectly using the pilots transmitted from the user. The linear detector matrix $\mathbf{A}_{M\times K}$ depends on the channel condition. In a similar manner as in [2], by using the linear detector, the received signal is obtained by multiplying it with $\mathbf{A}^H$ as follows

$$\mathbf{r}=\mathbf{A}^H\mathbf{y}, \tag{16}$$

where the linear detector $\mathbf{A}=\dot{\mathbf{G}}$ ($\mathbf{A}=\mathbf{G}$ in [2]). Then the received vector after using the linear detector is given by

$$\mathbf{r}=\sqrt{p_u}\mathbf{A}^H\dot{\mathbf{G}}\mathbf{s}+\mathbf{A}^H\mathbf{n}. \tag{17}$$

For a given user k we have

$$r_k=\sqrt{p_u}\mathbf{a}_k^H\dot{\mathbf{g}}_k s_k+\sqrt{p_u}\sum_{i=1,i\neq k}^{K}\mathbf{a}_i^H\dot{\mathbf{g}}_i s_i+\mathbf{a}_k^H\mathbf{n}, \tag{18}$$

where $\mathbf{a}_k$ and $\dot{\mathbf{g}}_k$ are the kth columns of the matrices $\mathbf{A}$ and $\dot{\mathbf{G}}$, respectively. The noise plus interference term, which is the sum of the multiuser interference and additive white Gaussian noise (AWGN), is a random variable with zero mean and variance of $P_u\sum_{i=1}^{K}\left|\mathbf{a}_k^H\dot{\mathbf{g}}_i\right|^2+\|\mathbf{a}_k\|^2$ where we have assumed the AWGN variance is unity. Here we assume all users are perfectly power controlled to have the same power at the BS. The same as in [2], we assume further that the channel is ergodic so that each codeword spans a large (infinite) number of realizations of the small scale fading factor of $\dot{\mathbf{G}}$. The codeword here is a sequence of the user transmitted symbols. Then the ergodic achievable uplink rate of the kth user can be expressed as following function of the signal to interference and noise ratio (SINR) as

$$\begin{aligned}R_{P,k}&=E\left\{\log_2\left(1+\mathrm{SINR}_k\right)\right\}\\&=E\left\{\log_2\left(1+\frac{p_u\left|\mathbf{a}_k^H\dot{\mathbf{g}}_k\right|^2}{p_u\sum_{i=1,i\neq k}^{K}\left|\mathbf{a}_k^H\dot{\mathbf{g}}_i\right|^2+\|\mathbf{a}_k\|^2}\right)\right\},\end{aligned} \tag{19}$$

where the subscript "P" on "R" indicates perfect channel estimation ("IP" will mean the imperfect channel estimation). With MRC, $\mathbf{A}=\dot{\mathbf{G}}$ so we have $\mathbf{a}_k=\dot{\mathbf{g}}_k$. When considering the LSA effect, the achievable uplink rate of the kth user is

$$R_{P,k}^{\mathrm{mrc}}=E\left\{\log_2\left(1+\frac{p_u\|\dot{\mathbf{g}}_k\|^4}{p_u\sum_{i=1,i\neq k}^{K}\left|\dot{\mathbf{g}}_k^H\dot{\mathbf{g}}_i\right|^2+\|\dot{\mathbf{g}}_k\|^2}\right)\right\}. \tag{20}$$

Consequently, in a similar manner as in [2], with perfect CSI, Rayleigh fading, and $M\geq 2$, we also provide a lower bound of the uplink achievable rate from the kth user for MRC (counterpart to eq.(16) in [2]) as follows

$$\tilde{R}_{P,k}^{\mathrm{mrc}}=\left\{\log_2\left(1+\frac{p_u(M-1)\eta_k/M}{p_u\left(\sum_{i=1,i\neq k}^{K}\eta_i/M\right)+1}\right)\right\}\leq R_{P,k}^{\mathrm{mrc}}, \tag{21}$$

Here, we also consider the case that the transmit power of each user is scaled with M according to $p_u=\frac{E_u}{M}$ (E_u is fixed). Then the lower bound on the ergodic achievable uplink rate of the kth user when M is indefinitely large is

$$\tilde{R}_{P,k}^{\mathrm{mrc}}\to\log_2\left(1+E_u\eta_k/M\right),\quad M\to\infty. \tag{22}$$

TABLE 1. Results of the achievable rate of the ZF detector for the *k*th user.

	ZF	
Perfect CSI	$R_{P,k}^{\mathrm{zf}} = E\left\{\log_2\left(1+\frac{p_u}{\left[\left(\dot{\mathbf{G}}^H\dot{\mathbf{G}}\right)^{-1}\right]_{kk}}\right)\right\}$	(32)
	$\tilde{R}_{P,k}^{\mathrm{zf}} = \log_2\left(1+\frac{p_u}{E\left\{\left[\left(\dot{\mathbf{G}}^H\dot{\mathbf{G}}\right)^{-1}\right]_{kk}\right\}}\right)$	(33)
Imperfect CSI	$R_{IP,k}^{\mathrm{zf}} = E\left\{\log_2\left(1+\frac{p_u}{\left(\sum_{i=1}^{K}\frac{p_u\eta_i}{\eta_i p_u\tau+M}+1\right)\left[\left(\hat{\dot{\mathbf{G}}}^H\hat{\dot{\mathbf{G}}}\right)^{-1}\right]_{kk}}\right)\right\}$	(34)
	$\tilde{R}_{IP,k}^{\mathrm{zf}} = \log_2\left(1+\frac{\tau p_u(M-K)\eta_k^2/M^2}{(\tau p_u\eta_k/M+1)\sum_{i=1}^{K}\left(\frac{\eta_i/M}{\tau p_u\eta_i/M+1}\right)+\tau\eta_k/M+1/p_u}\right)$	(35)

B. ACHIEVABLE RATE ($M \to \infty$) WITH IMPERFECT CSI AT THE BS

Here, we consider the case in which the channel estimation is not perfect. The condition is the same as in Section III.B in [2]. We assume that the orthogonal pilot sequences with length of τ used by all K users can be represented by a $\tau \times K$ matrix $\sqrt{p_p}\mathbf{\Phi}$, which satisfies $\mathbf{\Phi}^H\mathbf{\Phi} = \mathbf{I}_K$, where $p_p \triangleq \tau p_u$. When considering the LSA effect, the $M \times \tau$ faded pilot signals that arrive at the BS can be expressed as

$$\mathbf{y}_p = \sqrt{p_p}\dot{\mathbf{G}}\mathbf{\Phi}^T + \mathbf{N}, \tag{23}$$

where $\mathbf{N}$ is an $M \times \tau$ AWGN matrix with i.i.d. zero-mean and unit variance complex Gaussian random variables. We use the minimum mean-square error (MMSE) method to estimate the channel as

$$\hat{\dot{\mathbf{G}}} = \frac{1}{\sqrt{p_p}}\mathbf{y}_p\mathbf{\Phi}^*\left(R_{\dot{\mathbf{G}}}^{-1} + \mathbf{\Phi}\mathbf{\Phi}^T\right)^{-1}, \tag{24}$$

where $K \times K$ matrix $R_{\dot{\mathbf{G}}} = E\left(\dot{\mathbf{G}}^H\dot{\mathbf{G}}\right) = \frac{1}{M}\boldsymbol{\eta}$ when M is large. In a similar manner in [2], (24) can be written as

$$\hat{\dot{\mathbf{G}}} = \left(\dot{\mathbf{G}} + \frac{1}{\sqrt{p_p}}\mathbf{W}\right)\left(\frac{M}{p_p}\boldsymbol{\eta}^{-1} + \mathbf{I}_K\right)^{-1} = \left(\dot{\mathbf{G}} + \frac{1}{\sqrt{p_p}}\mathbf{W}\right)\bar{\mathbf{D}}, \tag{25}$$

where $\mathbf{W} = \mathbf{N}\mathbf{\Phi}^*$ has i.i.d. complex Gaussian random elements with zero-mean and unit variance, and $\bar{\mathbf{D}} = \left(\frac{M}{p_p}\boldsymbol{\eta}^{-1} + \mathbf{I}_K\right)^{-1}$. We denote $\hat{\dot{\mathbf{g}}}_k$ as the kth column of $\hat{\dot{\mathbf{G}}}$. Denoting the channel estimation error $\mathcal{E}$ and we have

$$\hat{\dot{\mathbf{G}}} = \dot{\mathbf{G}} + \mathcal{E}. \tag{26}$$

It is straightforward to show that the elements of the ith column of $\mathcal{E}$ are RVs with zero means and variances $\frac{p_p\eta_k}{M+p_p\eta_k}$ [16], which will decrease the received signal to noise ratio (SNR) at the BS. The signal vector after using the linear detector is

$$\hat{\mathbf{r}} = \hat{\mathbf{A}}^H\left(\sqrt{p_u}\hat{\dot{\mathbf{G}}}s - \sqrt{p_u}\mathcal{E}\mathbf{s} + \mathbf{n}\right), \tag{27}$$

and the signal vector after using the linear detector of the kth user

$$\hat{r}_k = \sqrt{p_u}\hat{\mathbf{a}}_k^H\hat{\dot{\mathbf{g}}}_k s_k + \sqrt{p_u}\sum_{i=1,i\neq k}^{K}\hat{\mathbf{a}}_k^H\hat{\dot{\mathbf{g}}}_i s_i - \sqrt{p_u}\sum_{i=1}^{K}\hat{\mathbf{a}}_k^H\boldsymbol{\varepsilon}_i s_i + \hat{\mathbf{a}}_k^H\mathbf{n}, \tag{28}$$

where $\hat{\mathbf{a}}$, $\hat{\dot{\mathbf{g}}}_i$ and $\boldsymbol{\varepsilon}_i$ are the ith column of $\hat{\mathbf{A}}$, $\hat{\dot{\mathbf{G}}}$ and $\mathcal{E}$, respectively. After some mathematical manipulations, the ergodic achievable uplink rate of the kth user can be expressed as (29), as shown at the bottom of the next page.

Again, in a manner similar to that in [2], with imperfect CSI, Rayleigh fading, MRC processing, and for $M \geq 2$, we can derive the lower bound on the achievable uplink rate for the kth user as (30), as shown at the bottom of the next page.

If the the transmit power per user is set to $\frac{E_u}{\sqrt{M}}$ and M grows without bound, then we also can obtain

$$\tilde{R}_{IP,k}^{mrc} \to \log_2\left(1+\tau E_u^2\eta_k^2/M^2\right), \quad M \to \infty. \tag{31}$$

Here, we also provide the corresponding result expression for the ZF detector, which could be derived in an analogous way. These results of MRC and ZF detectors are summarized in TABLE I.

IV. STATISTICAL CHARACTERISTICS OF $\frac{\eta_k}{M}$ AND β_k

In previous sections, it was found that the main difference of sum-rate values of the conventional model and LSA model is embodied in η_k and β_k. In this section, the statistic characteristics of η_k and β_k are investigated.

In our proposed LSA model, the large scale fading attenuation coefficient η_{mk} is determined by the propagation path length and shadowing. In [1], [2], and [5], it was stated that the massive MIMO system is able to harden the channel, i.e. $(\mathbf{h}_k)^H(\mathbf{h}_k) =$ constant. After the channel hardening operation, the channel variations (small scale fading effect) are negligible over the frequency domain (or time delay domain) and mainly depend on large-scale fading in the time domain(space

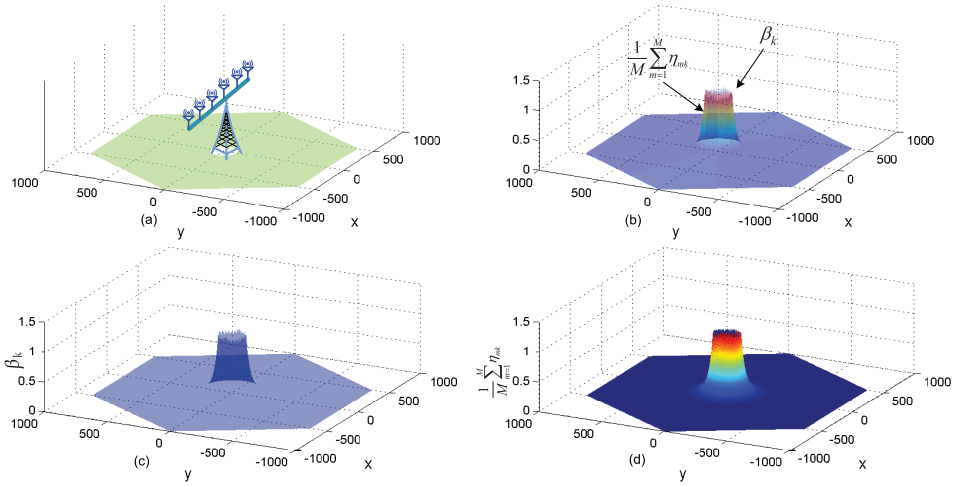

FIGURE 2. β_k and $\frac{1}{M}\sum_{m=1}^{M}\eta_{mk}$ in an $M = 128$ linear massive MIMO BS coverage area. (a). The wireless coverage area of an $M = 128$ linear massive MIMO BS coverage area; (b). The results of β_k and $\frac{1}{M}\sum_{m=1}^{M}\eta_{mk}$; (c). The results of β_k; (d). The results of $\frac{1}{M}\sum_{m=1}^{M}\eta_{mk}$.

domain), which typically varies 100-1000 times slower than the small-scale fading. From the conventional point of view, it was stated that the channel hardening effect means that the channel becomes more and more deterministic as the number of antennas grows. The variance of the random channel coefficient (small scale fading) tends to diminish with an increase in the number of antenna elements M. However, if we consider the LSA effect, some randomness still remains. In (8), the channel hardening effect in the conventional model means that the final hardening result is the large-scale channel coefficient, whereas, according to (11), this final effect when using the reference LSA model is the mean value of the sum of the large-scale channel coefficients from the active antenna elements over the antenna array. Here, we will consider two random factors: the distance r_{mk} causing individual power attenuation, and the shadowing effect x_{mk} on the kth user and mth antenna element propagation link.

In this section, we set up a single cell, a cell with a radius (from center to vertex) of 1000 meters, as the simulation environment. The users are located uniformly in the cell and we assume that no user is closer to the BS than $r_0 = 100$ meters, as shown in Figure 2 (a). The path loss exponent is $n = 3.8$.

A. NO SHADOWING AND USER IS NOMADIC

In the previous investigation, we found that the main difference between the conventional non-LSA model and the LSA model is the difference between $\frac{1}{M}(\mathbf{g}_k)^H(\mathbf{g}_l) \xrightarrow{M\to\infty} \beta_k$ and $\frac{1}{M}(\dot{\mathbf{g}}_k)^H(\dot{\mathbf{g}}_l) \xrightarrow{M\to\infty} \frac{1}{M}\sum_{m=1}^{M}\eta_{mk}$. We provide simulation results for β_k and $\frac{1}{M}\sum_{m=1}^{M}\eta_{mk}$ in an $M = 128$ linear massive MIMO example. Here, we assume first there is no shadowing effect, i.e. lognormal shadowing value $x = 1$. Figure 2 (b)-(d) illustrates the simulation results. It is obvious that the values of β_k (transparent shape) are essentially the same as those of $\frac{1}{M}\sum_{m=1}^{M}\eta_{mk}$ (colored shape), especially for the smaller link distances, as shown in Figure 2 (b). In order to see clearly, the fading results of β_k and $\frac{1}{M}\sum_{m=1}^{M}\eta_{mk}$ are provided separately, as shown in Figure 2 (c) and Figure 2 (d). From the separated figures, we can see that if the shadowing effects are not considered, the inner product results of channel vectors take approximately the same values when considering the LSA or not. Intuitively, we could guess that if the inner product of channel vectors changes, that would be caused by the

$$R_{IP,k}^{\mathrm{mrc}} = E\left\{\log_2\left(1+\frac{p_u\left\|\hat{\mathbf{g}}_k\right\|^4}{p_u\sum_{i=1,i\neq k}^{K}\left|\hat{\mathbf{g}}_k^H\hat{\mathbf{g}}_i\right|^2+p_u\left\|\hat{\mathbf{g}}_k\right\|^2\sum_{i=1}^{K}\frac{\eta_i}{M+\tau p_u\eta_i}+\left\|\hat{\mathbf{g}}_k\right\|^2}\right)\right\} \tag{29}$$

$$\tilde{R}_{IP,k}^{\mathrm{mrc}} = \log_2\left(1+\frac{\tau p_u(M-1)\eta_k^2/M^2}{(\tau p_u\eta_k/M+1)\sum_{i=1,i\neq k}^{K}(\eta_i/M)+(\tau+1)\eta_k/M+1/p_u}\right) \leq R_{IP,k}^{\mathrm{mrc}} \tag{30}$$

TABLE 2. LSA coefficients under different conditions.

Pure shadowing	
Conventional model	LSA model
$\beta^p = x$	$\frac{\eta^p}{M} = \frac{1}{M}\sum_{m=1}^{M} x_m$

Composite shadowing		
Conventional model	LSA model	ALSA model
$\beta_k = x \cdot \frac{(r_0)^n}{(r_k)^n}$	$\frac{\eta_k}{M} = \frac{(r_0)^n}{M}\sum_{m=1}^{M}\frac{x_{mk}}{(r_{mk})^n}$	$\frac{\eta_k^{ALSA}}{M} = \frac{(r_0)^n}{M(r_k)^n}\sum_{m=1}^{M} x_{mk}$

Note:
1. The first superscript p of β^p and $\frac{\eta^p}{M}$ stands for the "Pure shadowing" which means the case that where the attenuation caused by propagation distance differences across array elements is not considered. The "Composite shadowing" case is that which considers the propagation distance which causing the attenuation differences across array elements.
2. An "ALSA" model denotes the approximated LSA model. It corresponds to the case where the separation distance values between the user k and the individual antenna element values are approximately the same, i.e., $r_{1k} \approx r_{2k} \approx \cdots r_{Mk} \doteq r_k$. We can term this as a "far field" or large link distance ($d \gg$ length of array) condition.

shadowing effect. In the following section, we verify this hypothesis using the theoretical and simulation results.

B. INCLUSION OF SHADOWING

As for the shadowing effect on different antenna elements, we consider that the shadowing values on each of the M BS elements are independently distributed. It is easy but an ideal case which would require very large physical antenna size and element separation to be realistic. The correlated shadowing effects on different elements are considered in our future work. The use of this idealized reference model with independent shadowing will be shown to provide a useful bound to the practical correlated case.

We consider statistical properties of four parameters as shown in Table II. We assume that the mean value and the standard deviation of the shadowing effect (X) are $\mu = 0$ and $\sigma = 8$ dB, respectively.

(1). Pure shadowing

Proposition : If x_m are i.i.d, then $E(\beta^p) = E\left(\frac{\eta^p}{M}\right) = \exp\left[\frac{\mu}{\xi} + \frac{1}{2}\left(\frac{1}{\xi}\right)^2\sigma^2\right]$.[2]

Figure 3 (a) plots the probability density function (PDF) of β^p and $\frac{\eta^p}{M}$ (pure shadowing) associated with various values of M. As shown, when M grows, the range that the PDF spans becomes smaller and converges to the mean value $\exp\left[\frac{\mu}{\xi} + \frac{1}{2}\left(\frac{1}{\xi}\right)^2\sigma^2\right] = 5.45$ ($\mu = 0, \sigma = 8$). We term the number of antenna elements M the shadowing order. Figure 3 (b) plots the PDFs of $\log_2(\beta^p)$ and $\log_2\left(\frac{\eta^p}{M}\right)$ (pure shadowing) associated with various values of M. The PDF curves move right when M increases. After some mathematical operation, we can obtain $\log_2(\beta^p) = \log_2(x) = \frac{\log_2 10}{10}X$, and hence, $\log_2(x)$ follows the Gaussian distribution, as shown in Figure 3 (b). As for $\frac{\eta^p}{M} = \frac{1}{M}\sum_{m=1}^{M} x_m$, this term also follows the log-normal distribution.[3] Hence, $\log_2\left(\frac{\eta^p}{M}\right)$ is a variable following the Gaussian distribution, and the mean value of $\log_2\left(\frac{\eta^p}{M}\right)$ increases with the number of antenna elements M, but not grows when M is extremely large.

As shown in Figure 3 (b), the PDF shifts right and the span becomes smaller when M grows. The values, β^p and $\frac{\eta^p}{M}$, have different PDF shapes, i.e., the PDF of β^p spreads more than the PDF of $\frac{\eta^p}{M}$ with large M (see Figure 3 (a)). We can see more possible values occur between the range (0, $\exp\left[\frac{\mu}{\xi} + \frac{1}{2}\left(\frac{1}{\xi}\right)^2\sigma^2\right]$). When taking log function $\log_2(\cdot)$ on these variables, the mean values will increase with M, and take a larger value if the PDF span is smaller. Due to the fact that the sum rate value is a function of β_k and η_k in the conventional model and LSA model, respectively, it can be supposed that the mean value of the sum rate using the ideal reference LSA model might be larger than that derived from the conventional model.

Figure 4 plots the mean value of β^p, $\frac{\eta^p}{M}$, $\log_2(\beta^p)$ and $\log_2\left(\frac{\eta^p}{M}\right)$ for different values of M. This figure supports the previous *Proposition* and shows the mean values of β^p

[2] If $X \sim N(\mu, \sigma^2)$, then the moments of $x = 10^{0.1X}$ are given by $E[x^k] = \exp\left[\frac{k}{\xi}\mu + \frac{1}{2}\left(\frac{k}{\xi}\right)^2\sigma^2\right]$ ($\xi = 10/\ln 10$), and the mean and variance value are $\exp\left[\frac{\mu}{\xi} + \frac{1}{2}\left(\frac{1}{\xi}\right)^2\sigma^2\right]$ and $\exp\left[2\mu + \sigma^2\right]\left[\exp\left(\sigma^2\right) - 1\right]$, respectively [17]. Because x_m are i.i.d, we can easily obtain $E\left(\frac{\eta^p}{M}\right) = \exp\left[\frac{\mu}{\xi} + \frac{1}{2}\left(\frac{1}{\xi}\right)^2\sigma^2\right]$

[3] It has been stated that a sum of log-normal random variables can be well approximated by another log-normal random variable [18] and [19].

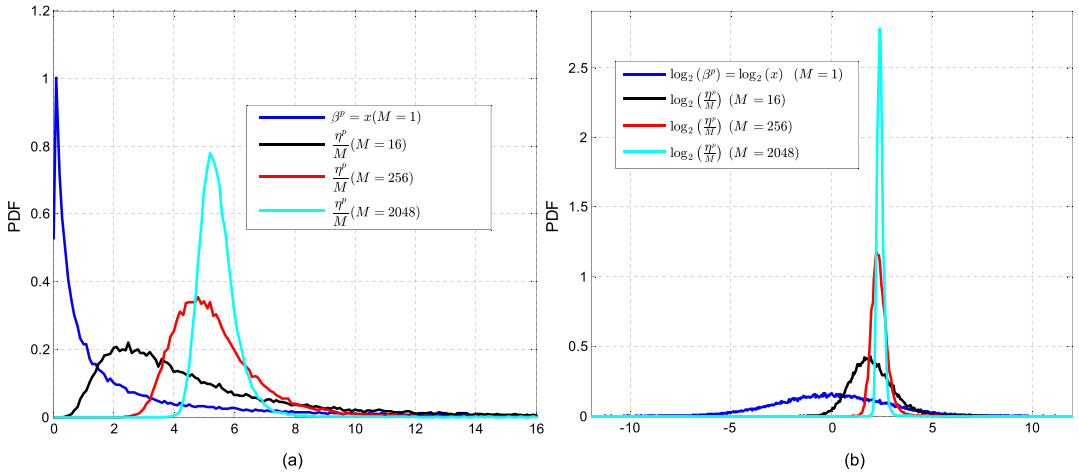

FIGURE 3. PDF values of β^p, $\frac{\eta_k^p}{M}$, $\log_2(\beta^p)$ and $\log_2\left(\frac{\eta_k^p}{M}\right)$ for different values of M.

and $\frac{\eta_k^p}{M}$ (blue lines) approximate $\exp\left[\frac{\mu}{\xi}+\frac{1}{2}\left(\frac{1}{\xi}\right)^2\sigma^2\right] = 5.45$. Meanwhile, we compare the mean values of two simple functions, $E\left(\log_2(\beta^p)\right)$ and $E\left(\log_2\left(\frac{\eta_k^p}{M}\right)\right)$. It can be found that $E\left(\log_2\left(\frac{\eta_k^p}{M}\right)\right)$ increases with the number of antenna elements M, whereas, $E\left(\log_2(\beta^p)\right)$ remains constant. Since (22) indicates that the sum rate grows with $E\left(\log_2\left(\frac{\eta_k^p}{M}\right)\right)$, the hypothesis that the achievable rate using the reference LSA model may be larger than the value using the conventional model is thus verified this case.

Importantly, it can be inferred that when the number of antenna elements M tends to infinity, the PDFs of $\frac{\eta_k^p}{M}$ will converge to a Dirac delta function located at $\exp\left[\frac{\mu}{\xi}+\frac{1}{2}\left(\frac{1}{\xi}\right)^2\sigma^2\right]$, as shown in Figure 3 (a). The same as the PDF of $\frac{\eta_k^p}{M}$, it appears that the PDF of $\log_2\left(\frac{\eta_k^p}{M}\right)$ also converges to a Dirac delta function as M tends to infinity. This means the mean value of $\log_2\left(\frac{\eta_k^p}{M}\right)$ is reaching a limit (maximum) value $\log_2\left(\exp\left[\frac{\mu}{\xi}+\frac{1}{2}\left(\frac{1}{\xi}\right)^2\sigma^2\right]\right) = 2.4463$ $(\mu=0, \sigma=8)$ when M grows infinitely large, as shown the red line in Figure 4.

(2). Composite shadowing

Figure 5 plots the mean values of β_k, $\frac{\eta_k}{M}$, $\frac{\eta_k^{ALSA}}{M}$, $\log_2(\beta_k)$, $\log_2\left(\frac{\eta_k}{M}\right)$ and $\log_2\left(\frac{\eta_k^{ALSA}}{M}\right)$ with different number of antenna elements M. We consider the geometrical effects here. Similar conclusions results:

- The mean values of β_k, $\frac{\eta_k}{M}$ and $\frac{\eta_k^{ALSA}}{M}$ do not change with M. Most importantly, we can see that the mean values of $\frac{\eta_k}{M}$ and $\frac{\eta_k^{ALSA}}{M}$ are approximately the same, and mean values of $\log_2\left(\frac{\eta_k}{M}\right)$ and $\log_2\left(\frac{\eta_k^{ALSA}}{M}\right)$ approximate the same.

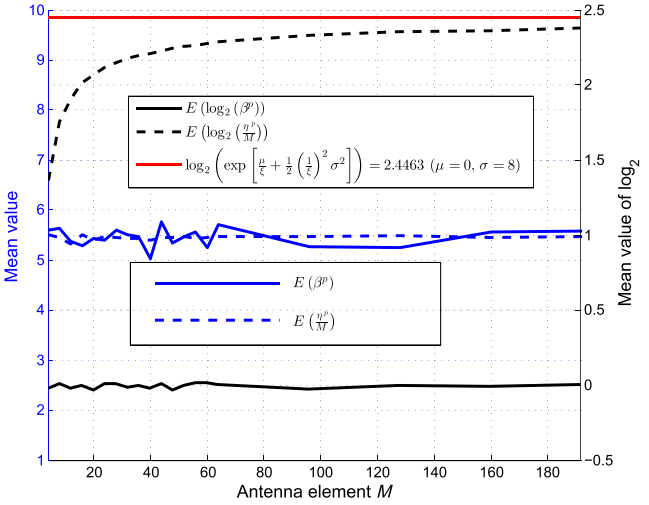

FIGURE 4. Mean values of β^p, $\frac{\eta_k^p}{M}$, $\log_2(\beta^p)$ and $\log_2\left(\frac{\eta_k^p}{M}\right)$ versus M.

- The same as for the pure shadowing results, the mean values of $\log_2\left(\frac{\eta_k}{M}\right)$ increase with the number of antenna elements M ($\log_2\left(\frac{\eta_k}{M}\right)$ has a maximum value when M is indefinitely large), whereas, the values of β_k and $\frac{\eta_k}{M}$ remain the same. The reason for this could be attributed to the non-linear property of the Log function $\log_2(\cdot)$. The mean value of the case considering the different shadowing effect grows with the number of antenna elements M.

(3). Effect of the standard deviation σ

Figure 6 provides the distributions of $\log_2\left(\frac{\eta_k^p}{M}\right)$ for different standard deviation σ when $M = 256$. It can be found that the PDF curves move right and spread more with σ. Based on these results it is reasonable to suppose that the mean values of $\log_2\left(\frac{\eta_k^p}{M}\right)$ will increase with larger standard deviation. By using our proposed LSA model, it can be assumed that

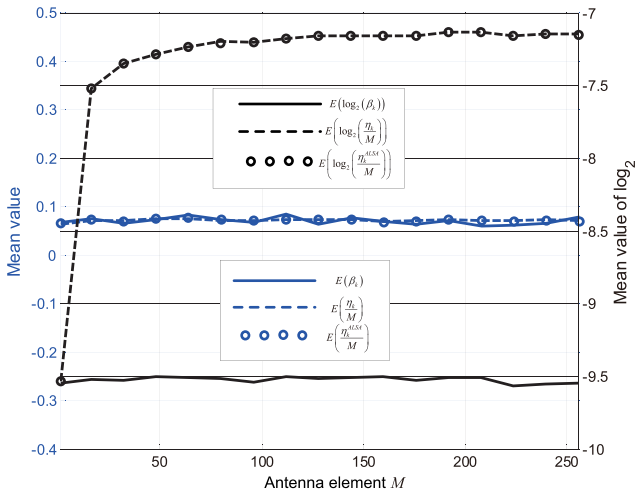

FIGURE 5. Mean values of β_k, $\frac{\eta_k}{M}$, $\frac{\eta_k^{ALSA}}{M}$, $\log_2(\beta_k)$, $\log_2\left(\frac{\eta_k}{M}\right)$ and $\log_2\left(\frac{\eta_k^{ALSA}}{M}\right)$.

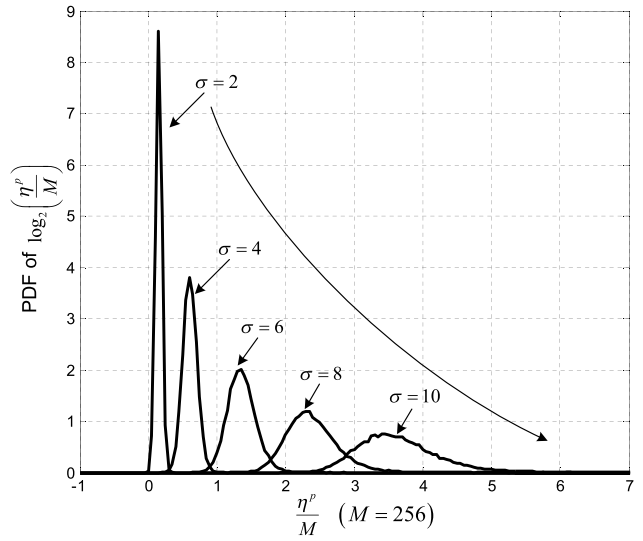

FIGURE 6. PDF of $\log_2\left(\frac{\eta^P}{M}\right)$ for different standard deviation σ when $M = 256$.

the sum-rate will increase if the propagation environment is bad, i.e., if the shadow standard deviation is large.

From the above investigation, due to the fact that the sum rate is a function of $\frac{\eta_k}{M}$ and β_k in the reference LSA model and the conventional model, respectively, we observe that

- The mean value of the sum rate value using the LSA model is larger than the value using the conventional model;
- From the channel hardening effect point of view, it is implied that the shadowing combining brings the performance benefit;
- The transmission performance will increase when the shadowing effect becomes more severe.

These results will be verified in the following section.

V. NUMERICAL RESULTS

In this section, numerical results are presented to examine the performance when considering the ideal reference LSA effect. We again consider a hexagonal cell with a radius (from center to vertex) of 1000 meters. The users are randomly located in the cell and we assume that no user is closer to the BS than $r_0 = 100$ meters. We assume that there are $K = 10$ users, the coherence interval $\tau = 196$, the transmit power per terminal is $p_u = 10dB$,[4] and the propagation channel parameters are $\sigma = 8$ dB, and $n = 3.8$. The simulation parameters are the same as the simulation parameters in [2].

Figure 7 separately plots the simulated results and lower bound results ((21) and (30)) of the achievable rate of $K = 10$ users with different numbers of the BS antennas M, under perfect and imperfect channel estimation conditions, respectively. We can obtain the following conclusions:

(1). The spectral efficiency results using the LSA model (both perfect CSI and imperfect CSI conditions) are larger than the results simulated using the conventional model, including MRC, ZF cases. The difference of the transmission performance is substantially large, exceeding 15 bits/s/Hz for $M = 500$. This is a huge performance gap. Hence, the conventional model may underestimate the transmission performance of a massive MIMO system if the LSA effect is not considered.

(2). Due to the large separation distance between the user and the antenna array (compared with the antenna size), we also provide the results (ALSA model) in which there are no path length differences among the propagation rays caused by the antenna size. Since results do not change from the reference LSA model, the large scale fading difference comes only from the individual shadowing effects from different antenna elements. These simulation results support our previous hypothesis. The performance improvement is from the independent shadowing fading.

We also provide simulation results using the LSA based conventional model which are in line with the results of the conventional model, both under the perfect and imperfect channel estimation conditions.

Figure 8 plots both the simulated and lower bound results of the achievable rate of $K = 10$ users vs. different standard deviation of the shadowing effect σ, under perfect and imperfect channel estimation condition. We set the number of antenna elements $M = 256$. The main results are as follows:

(1) The spectral efficiency increases with the standard deviation of the shadowing effect σ, both for the conventional model and ideal reference LSA model. Compared with the conventional model, the sum rate values of the reference LSA models increase more rapidly. The simulation results are in line with the results provided in Figure 6, i.e., the mean values of $\log_2\left(y_{LSA}^p\right)$ increase with the standard deviation σ. We can conclude that in the ideal reference LSA massive MIMO

[4]As mentioned in [2], *pu* has the interpretation of normalized transmit SNR, and it is dimensionless.

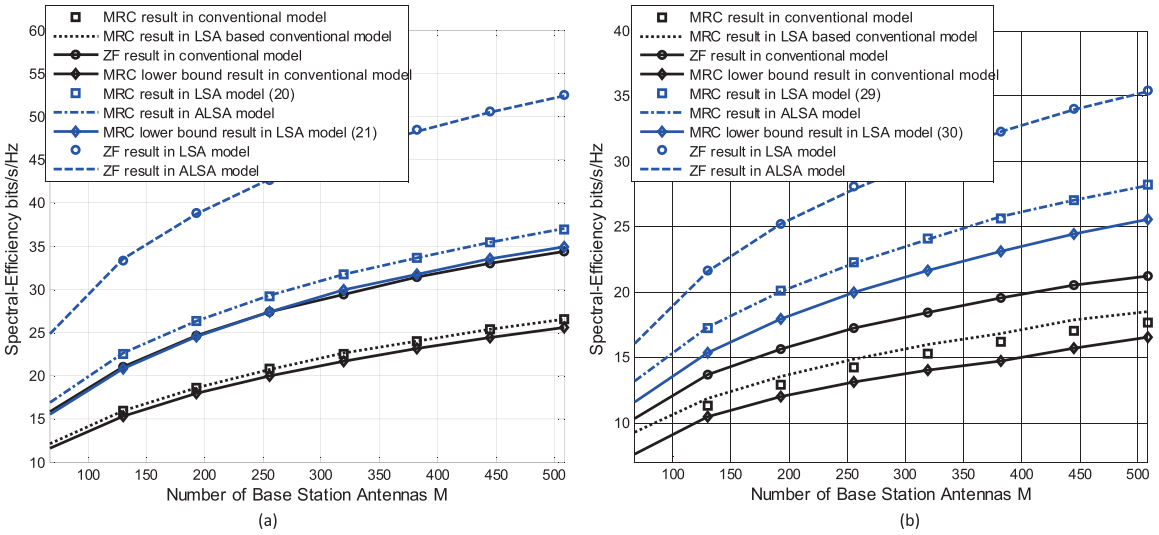

FIGURE 7. The spectral efficiency results v.s. the number of antenna elements. (a) The channel estimation is perfect. (b). The channel estimation is not imperfect.

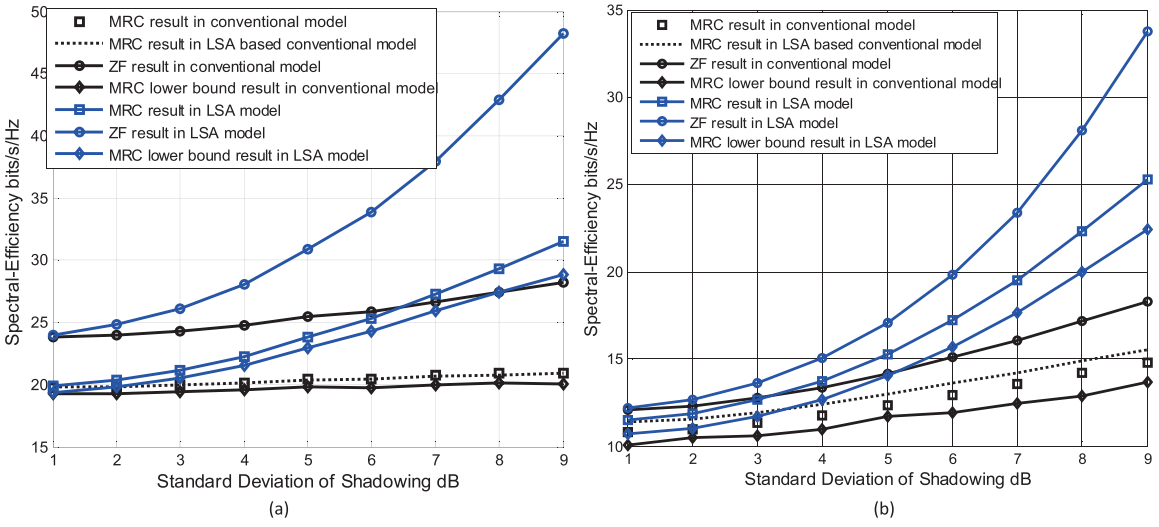

FIGURE 8. The spectral efficiency results v.s. shadowing standard deviation. (a) The channel estimation is perfect. (b). The channel estimation is not imperfect.

propagation environment, a stronger shadowing effect can improve the transmission efficiency.

(2) When the shadowing effect σ is the same, we can find that the spectral efficiency value using the ideal reference LSA model is larger than the value using the conventional model.

Finally, the simulation results considering the power scaling laws are provided. Figure 9 shows the spectral efficiency on the uplink versus the number of BS antennas for $p_u = \frac{E_u}{M}$ and $p_u = \frac{E_u}{\sqrt{M}}$ with perfect and imperfect receiver CSI, and with MRC and ZF processing, respectively. The same as in [2], we choose $E_u = 20\ dB$. As expected (Figure 9 (a)), with $p_u = \frac{E_u}{M}$, when M increases, the spectral efficiency in the conventional model approaches a constant value for the case of perfect CSI, but decreases to 0 for the case of imperfect CSI (the same as results provided in [2]), and the spectral efficiency results in the ideal reference LSA model have the similar tendencies. However, the results using the ideal reference LSA model are larger than the counterpart results using the conventional model. The transmission gaps of perfect CSI and imperfect CSI cases tend toward 4.5 bps and 1.5 bps, respectively. As for the $p_u = \frac{E_u}{\sqrt{M}}$ condition, for the case of perfect CSI the spectral efficiency grows without bound when $M \to \infty$ (We can easily obtain the achievable uplink rate $\tilde{R}_{P,k}^{\text{mrc}} \xrightarrow{M\to\infty} \log_2\left(1+\sqrt{M}E_u\eta_k\right)$ for the kth user when $p_u = \frac{E_u}{\sqrt{M}}$), and with imperfect CSI, the spectral efficiency converges to a nonzero limit as $M \to \infty$. Results using the conventional model and ideal reference LSA model also follow this tendency. Again, results from

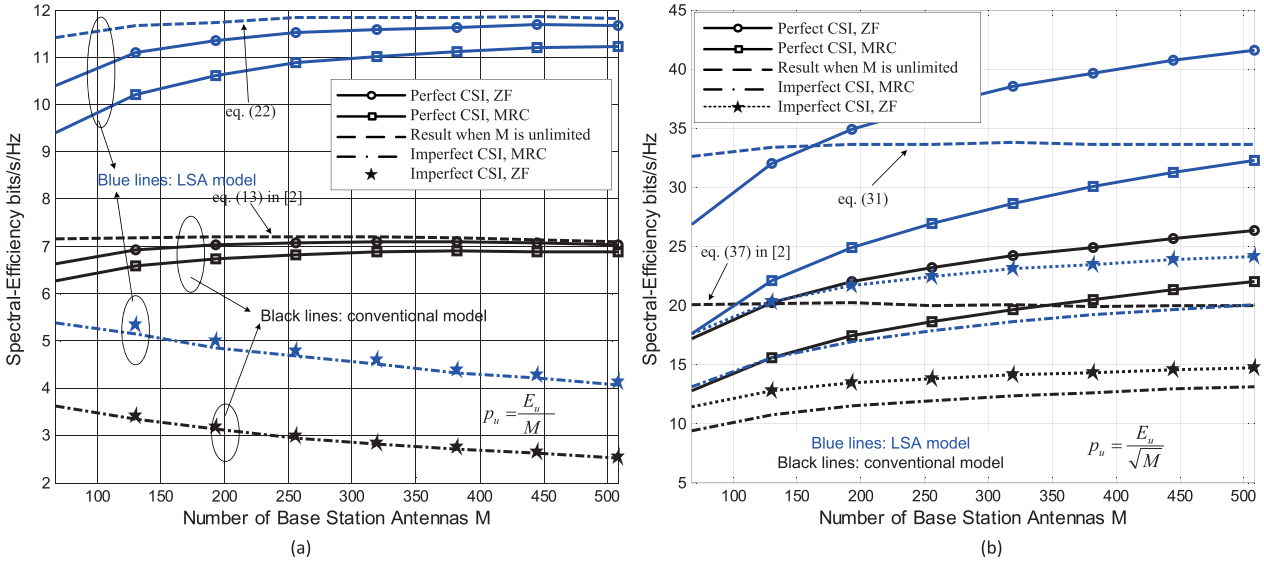

FIGURE 9. The average ergodic achievable rate of all the users with different number of BS antennas M considering the two different large scale models.

the ideal reference LSA model are larger than the results from the conventional model. Simulation results from our proposed LSA model also confirm that we can scale down the transmitted power of each user as $\frac{E_u}{M}$ for the perfect CSI case, and as $\frac{E_u}{\sqrt{M}}$ for the imperfect CSI case when M is large.

VI. CONCLUSIONS

A massive MIMO system having a large number of antenna elements is likely to be an emerging system that can significantly improve the frequency and power efficiency of future wireless systems. In the conventional channel model, the spectral efficiency (in terms of bits/s/Hz sum-rate) is mainly determined by the large scale fading characteristics of the channel when the number of antenna elements is infinitely large. However, previous research results largely neglect the effects of large-scale fading, and this conventional model does not consider the different power loss and shadowing effects across the antenna array. When considering an ideal reference LSA effect along the antenna array with independent shadowing across elements, though it is not practical, we can find the spectral efficiency results are larger than the values derived from the conventional model. Using our analytical method, the result of ZF receiver was obtained. From the investigation, we found that

(1) The spectral efficiency results using the ideal reference LSA model are substantially larger than the results simulated using the conventional model, including MRC, ZF and the result when we assume M is indefinitely large. In this paper, the spectral efficiency results (in terms of bits/s/Hz sum-rate) of the MRC under the perfect and imperfect channel estimation conditions were derived.

(2) The power loss difference over the antenna array caused by the propagation link has little effect on the spectral efficiency result. The performance gap mainly derives from the sum of the different shadowing samples from individual antenna elements.

(3) The spectral efficiency values of the conventional and ideal reference LSA model also increase with the standard deviation of the shadowing. In the ideal reference LSA massive MIMO propagation environment, a strong shadowing propagation environment can improve the transmission efficiency.

These findings are informative to the design and evaluation of the system performance using the massive MIMO technique. Future work will consider more realistic correlated shadowing across the array.

REFERENCES

[1] F. Rusek *et al.*, "Scaling up MIMO: Opportunities and challenges with very large arrays," *IEEE Signal Process. Mag.*, vol. 30, no. 1, pp. 40–60, Jan. 2013.

[2] H. Q. Ngo, E. G. Larsson, and T. L. Marzetta, "Energy and spectral efficiency of very large multiuser MIMO systems," *IEEE Trans. Commun.*, vol. 61, no. 4, pp. 1436–1449, Apr. 2013.

[3] H. Yang and T. L. Marzetta, "Performance of conjugate and zero-forcing beamforming in large-scale antenna systems," *IEEE J. Sel. Areas Commun.*, vol. 31, no. 2, pp. 172–179, Feb. 2013.

[4] H. Q. Ngo, E. G. Larsson, and T. L. Marzetta, "Aspects of favorable propagation in massive MIMO," in *Proc. 22nd Eur. Signal Process. Conf. (EUSIPCO)*, Bristol, U.K., Sep. 2014, pp. 76–80.

[5] E. Björnson, E. G. Larsson, and T. L. Marzetta, "Massive MIMO: Ten myths and one critical question," *IEEE Commun. Mag.*, vol. 54, no. 2, pp. 114–123, Feb. 2016.

[6] A. Chockalingam and B. S. Rajan, *Large MIMO Systems*. Cambridge, U.K.: Cambridge Univ. Press, Jun. 2014.

[7] F. Tufvesson, "Very large MIMO systems ICASSP, tutorial—-Part II: Propagation aspects of very large MIMO," in *Proc. 37th IEEE Int. Conf. Acoust., Speech, Signal Proccess. (ICASSP)*, 2012.

[8] S. Payami and F. Tufvesson, "Channel measurements and analysis for very large array systems at 2.6 GHz," in *Proc. 6th Eur. Conf. Antennas Propag. (EUCAP)*, Prague, Czech Republic, Mar. 2012, pp. 433–437.

[9] E. G. Larsson, O. Edfors, F. Tufvesson, and T. L. Marzetta, "Massive MIMO for next generation wireless systems," *IEEE Commun. Mag.*, vol. 52, no. 2, pp. 186–195, Feb. 2014.
[10] L. Liu, D. W. Matolak, C. Tao, Y. Lu, B. Ai, and H. Chen, "Geometry based large scale attenuation over linear massive MIMO systems," in *Proc. 10th Eur. Conf. Antennas Propag. (Eucap)*, Apr. 2016, pp. 1–5.
[11] S. Payami and F. Tufvesson, "Delay spread properties in a measured massive MIMO system at 2.6 GHz," in *Proc. IEEE 24th Int. Symp. Pers. Indoor Mobile Radio Commun. (PIMRC)*, London, U.K., Sep. 2013, pp. 53–57.
[12] X. Gao, M. Zhu, F. Rusek, F. Tufvesson, and O. Edfors, "Large antenna array and propagation environment interaction," in *Proc. 48th Annu. Asilomar Conf. Signals, Syst., Comput.*, Pacific Grove, CA, USA, Nov. 2014, pp. 666–670.
[13] X. Gao, O. Edfors, F. Rusek, and F. Tufvesson, "Massive MIMO performance evaluation based on measured propagation data," *IEEE Trans. Wireless Commun.*, vol. 14, no. 7, pp. 3899–3911, Jul. 2015.
[14] A. Yang, Z. He, C. Xing, Z. Fei, and J.-M. Kuang, "The role of large-scale fading in uplink massive MIMO systems," *IEEE Trans. Veh. Technol.*, vol. 65, no. 1, pp. 477–483, Jan. 2015.
[15] A. F. Molisch, *Wireless Communications*, 2nd ed. Chichester, U.K.: Wiley, Apr. 2011.
[16] M. Biguesh and A. B. Gershman, "Training-based MIMO channel estimation: A study of estimator tradeoffs and optimal training signals," *IEEE Trans. Signal Process.*, vol. 54, no. 3, pp. 884–893, Mar. 2006.
[17] M. K. Simon and M.-S. Alouini, *Digital Communication Over Fading Channels*, 2nd ed. New York, NY, USA: Wiley, Nov. 2004.
[18] L. Fenton, "The sum of log-normal probability distributions in scatter transmission systems," *IRE Trans. Commun. Syst.*, vol. 8, no. 1, pp. 57–67, Mar. 1960.
[19] S. C. Schwartz and Y. S. Yeh, "On the distribution function and moments of power sums with log-normal components," *Bell Syst. Tech. J.*, vol. 61, no. 7, pp. 1441–1462, Sep. 1982. [Online]. Available: http://dx.doi.org/10.1002/j.1538-7305.1982.tb04353.x

LIU LIU received the B.E. and Ph.D. degrees from Beijing Jiaotong University, Beijing, China, in 2004 and 2010, respectively. From 2010 to 2012, he was a Post Ph.D. Researcher with the School of Electronics and Information Engineering, Institute of Broadband Wireless Mobile Communications, Beijing Jiaotong University, where he has been an Associated Professor since 2012. His general research interests include channel measurement and modeling for different propagation environments and signal processing of wireless communication in time-varying channel.

DAVID W. MATOLAK (S'82–M'83–SM'00) received the B.S. degree from Pennsylvania State University, University Park, the M.S. degree from the University of Massachusetts, Amherst, and the Ph.D. degree from the University of Virginia, Charlottesville, all in electrical engineering. He was with the Rural Electrification Administration, the UMass LAMMDA Laboratory, AT&T Bell Laboratories Microwave Radio Systems Development Department, the University of Virginia's Communication Systems Laboratory, Lockheed Martin Tactical Communication Systems, MITRE Corp., and Lockheed Martin Global Telecommunications. This work in industry addressed point to point/multipoint and mobile radio for terrestrial, satellite, and aeronautical communication systems for both civil and military applications. He spent 13 years with the School of Electrical Engineering and Computer Science, Ohio University. In 2012, he joined the Department of Electrical Engineering, University of South Carolina, Columbia, SC. His research interests are communication over fading channels, radio channel modeling, multicarrier transmission, and mobile ad hoc networks. He is a member of Eta Kappa Nu and Sigma Xi. He has served on numerous IEEE conference and technical program committees. He was the Chair of the Geo Mobile Radio Standards Group in the Telecommunications Industries Association's Satellite Communications Division. He is an Editor of the IEEE TRANSACTIONS ON VEHICULAR TECHNOLOGY.

CHENG TAO received the M.S. degree in telecommunication and electronic system from Xidian University, Xian, China, in 1989, and the Ph.D. degree in telecom-munication and electronic system from Southeast University, Nanjing, China, in 1992. From 1993 to 1995, he was a Post-Doctoral Fellow with the School of Electronics and Information Engineering, Beijing Jiaotong University (BJTU), Beijing, China. From 1995 to 2006, he was with the Air Force Missile College and the Air Force Commander College.

In 2006, he joined the Academic Faculty of BJTU, where he is currently a Full Professor and the Director of the Institute of Broadband Wireless Mobile Communications. He has authored over 50 papers and holds 20 patents. His research interests include mobile communications, multiuser signal detection, radio channel measurement and modeling, and signal processing for communications.

YONGZHI LI received the B.E. degree from Beijing Jiaotong University (BJTU), Beijing, China, in 2012, where he is currently pursuing the Ph.D. degree. From 2013 to 2014, he was the Chair of the China Institute of Communications, BJTU Student Branch. His current research interests include massive MIMO and signal processing in wireless communication.